Comparisons of Flow Patterns over a Hierarchical and a Non-hierarchical Surface in Relation to Biofouling Control

Mohammed Ridha Bin Ahmad Fawzan[1] and *Felicia* Wong Yen Myan[1,*]

1Department of Mechanical Engineering, School of Engineering, Taylor's University, 1, Jalan Taylors, 47500 Subang Jaya, Selangor, Malaysia.

Abstract. Biofouling can be defined as unwanted deposition and development of organisms on submerged surfaces. It is a major problem as it causes water contamination, infrastructures damage and increase in maintenance and operational cost especially in the shipping industry. There are a few methods that can prevent this problem. One of the most effective methods which is using chemicals particularly Tributyltin has been banned due to adverse effects on the environment. One of the non-toxic methods found to be effective is surface modification which involves altering the surface topography so that it becomes a low-fouling or a non-stick surface to biofouling organisms. Current literature suggested that non-hierarchical topographies has lower antifouling performance compared to hierarchical topographies. It is still unclear if the effects of the flow on these topographies could have aided in their antifouling properties. This research will use Computational Fluid Dynamics (CFD) simulations to study the flow on these two topographies which also involves comparison study of the topographies used. According to the results obtained, it is shown that hierarchical topography has higher antifouling performance compared to non-hierarchical topography. This is because the fluid characteristics at the hierarchical topography is more favorable in controlling biofouling. In addition, hierarchical topography has higher wall shear stress distribution compared to non-hierarchical topography

1 Introduction

Biofouling is any unwanted deposition and development of organisms on submerged surfaces [1]. It is a major problem as it contaminates water and medical instruments inflicting health risk. Biofouling also causes unnecessary drag leading to low fuel efficiency of marine industry and reduces operational range. Other than that, biofouling promotes physical damage to infrastructures resulting in increased maintenance cost [2]. US$2.3 million were spent annually on a vessel due to biofouling of the vessel hull which causes increase in fuel consumption by 20.4% due to drag [3]. In oil and gas sector, the cost to

* Corresponding author: feliciayenmyan.wong@taylors.edu.my

repair equipment damaged by biofouling is approximately US$ 960 to US$ 1280 million [4]. These examples show that it is important for researchers to develop antifouling measures to control this problem.

T. Vladkova [2] explained in her study that there are three principles to control biofouling. The first is to use the mechanical approach to detach the biofoulers from the surface. The second approach is the application of chemical agents to exterminate or inactivate the biofouling organisms. The last approach is surface modification which involves altering either surface chemical composition or surface topography so that it becomes a low-fouling or non-stick surface to biofouling organisms [5]. Rosenhahn et al. [6] also recommended similar approach which include toxic antifouling coatings, fouling release coating and foul release via surface modification as shown in Figure 1.

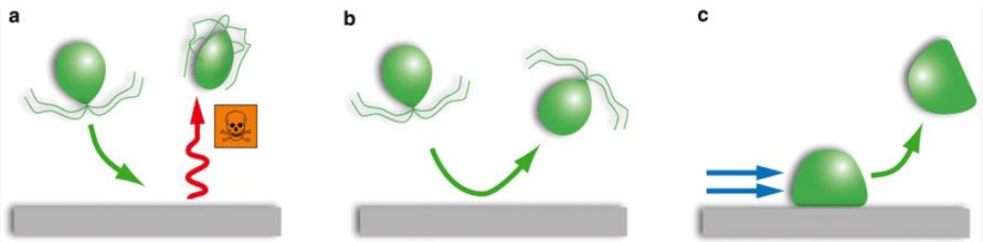

Fig. 1. Approaches to prevent biofouling: (a) toxic antifouling, (b) foul release, (c) foul inhibition [6]

A variety of chemical approaches were used to prevent biofouling of surfaces and some of it has been banned because of its adverse effects on the environment. Decades ago, a type of biocide named Tributyltin (TBT) was used as a coating on vessel hulls to prevent biofouling and by far this is the most effective method to mitigate biofouling in the history of antifouling technology to date [7]. However, this method was banned by the International Maritime Organisation (IMO) in November 2001. This is because IMO discovered that TBT causes detrimental effects on the environment like abnormal growth of the oysters, imposex (female gastropods developing male characteristics) and others [8–10]. K. A. Dafforn [7] also mentioned about the usage of copper as a co-biocide to increase the efficacy of TBT in paints for vessel hulls [11]. Copper is essential for metabolic functioning but it becomes toxic when the bioavailability level of copper exceeds the tolerance level of an organism [12]. The adverse effects of copper on the environment also eventually lead to restrictions of copper usage in paints for vessel hulls in countries like Canada, Denmark and the United States [13]. These were two popular chemical approaches that were used to control biofouling.

As mentioned above, surface modification is another method that can be used for antifouling applications. This method is preferable over other chemical approaches because it is environmental friendly. Previous studies have investigated the effects of surface topographies modification and the results are promising. The surface topographies' modification includes modifying the size and geometry. In recent years, these studies apply Computational Fluid Dynamics (CFD) to study the flow of the fluid on top of these modified surfaces [14]. By studying the flow, researchers can better ascertain the optimum size and geometry of surface topographies that can control biofouling effectively. More studies using this method is needed because it is relatively new compared to other methods and also to measure its efficacy for antifouling applications.

2 Research Methodology

2.1 Geometry Modeling

Solidworks 2013 was used in creating the fluid domain. The fluid domain consists of a rectangular block as shown in Figure 2 with a length of 80 mm and a square cross section of width and height of 8 mm. The distance between the inlet of the fluid domain and the topography array is 65 mm. The creation and placement of the array nearby outlet follows the Hagen-Poiseuille's flow theory [15]. This theory explains that in a fluid will develop a laminar flow in any fluid domain with a very significant difference in length compared to the size of its cross section. The development of the laminar flow is induced by the pressure drop along the flow. Two models were created for this research.

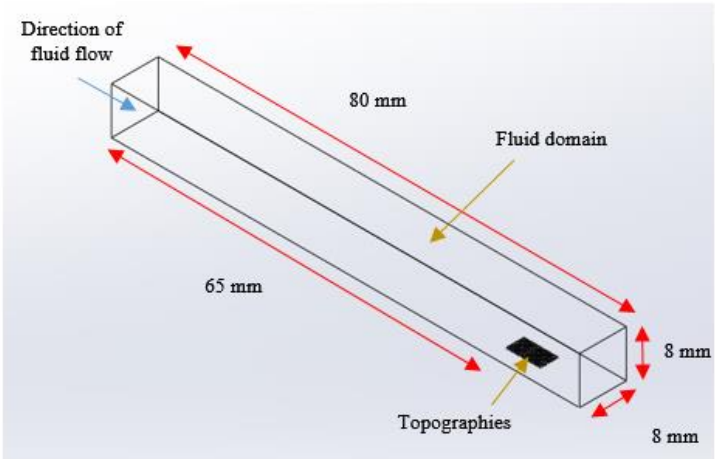

Fig 1. Dimensions of the fluid domain and the location of the topography array in the fluid domain.

Figure 3 shows a close up view of non-hierarchical topography while Figure 4 shows close up view of hierarchical topography with circular pillars. The selection of the geometry and size for these topographies are based on the literature.

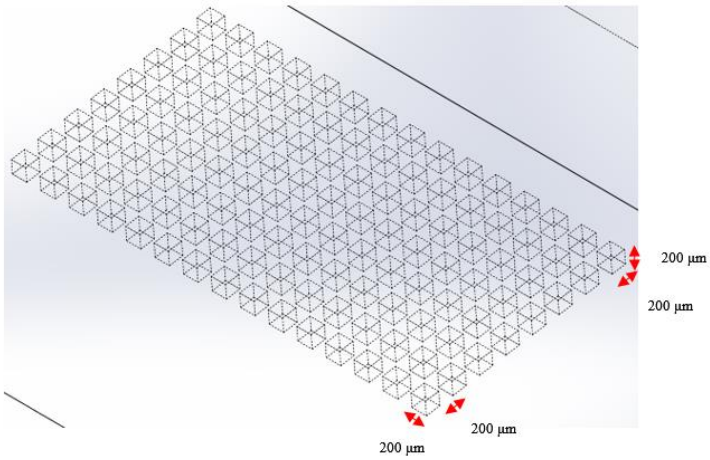

Fig. 3. Dimensions of the non-hierarchical topography

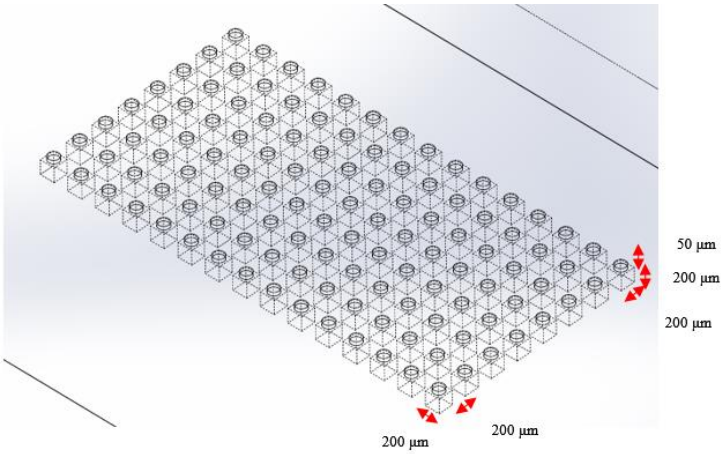

Fig. 2. Dimensions of hierarchical topography

Halder et al. [14] , the author found that well circumscribed geometries like circle, rectangle, hexagon and others develops higher shear bounded isolated areas compared to continuous geometries like ridges. Hence, cube was chosen as the first layer for non-hierarchical topography. Circular pillar was chosen as another well circumscribed geometry for the second layer of the topography to develop hierarchical topography. According to Nick Aldred et al. [16], the optimum size of topography to control biofouling is between 64-256 µm. Most of the biofouling organisms failed to attach to the surface at this range of size [16]. Therefore, all dimensions used in this research are within this range as shown in Figure 3 and 4

2.2 Meshing Method

The quality of the meshes on all models must be assessed to preserve the accuracy of the simulations. Models created using Solidworks were exported as STEP format files into ANSYS. Then, the meshing module was opened to start the meshing process. A fine mesh was created with tetrahedral elements and a sample is shown in Figures 5.

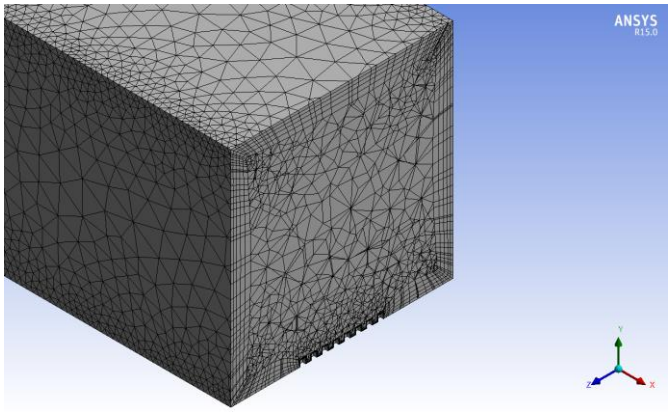

Fig. 5. Close up view of the meshing around the topography.

2.3 Boundary and Numerical Setup

The boundary and numerical setup for the research was done using CFD software package ANSYS FLUENT, version 15. The fluid used for this simulation is water with density ρ, of 1000 kgm^{-3} and dynamic viscosity μ, of 0.00001 $kgm^{-1}s^{-1}$. The k-ω turbulence model was used to simulate the flow as this model is able to provide higher accuracy of wall shear results [14]. The wall of the fluid domain was set with no-slip boundary condition. According to the study done by Halder et al. [14], the mass flow rate was set at 0.001 kgs^{-1} at the inlet and outlet. It is important to note that the mass flow rate was set faster than Halder's study as the model used in this research is longer and has larger cross section [14].

The Navier-Stokes equations (Equation 1 to 3) and the continuity equation (Equation 4) was used in this flow study. The continuity equation ensures the conservation of mass and momentum [17].

$$\frac{\partial \rho \mathbf{u}}{\partial t} + \nabla \cdot \rho \mathbf{u} V = -\frac{\partial \rho}{\partial x} + \nabla \cdot (\mu \nabla \mathbf{u}) + S_{m,x} \tag{1}$$

$$\frac{\partial \rho \mathbf{v}}{\partial t} + \nabla \cdot \rho \mathbf{v} V = -\frac{\partial \rho}{\partial y} + \nabla \cdot (\mu \nabla \mathbf{v}) + S_{m,y} \tag{2}$$

$$\frac{\partial \rho \mathbf{w}}{\partial t} + \nabla \cdot \rho \mathbf{w} V = -\frac{\partial \rho}{\partial z} + \nabla \cdot (\mu \nabla \mathbf{w}) + S_{m,z} \tag{3}$$

$$\frac{\partial \rho \mathbf{u}}{\partial t} + \nabla \cdot (\rho V) = 0 \tag{4}$$

Where *u, v* and *w* represents the velocity in *x, y* and *z* direction, ρ and μ are the fluid density and dynamic viscosity, *V* is the velocity and $S_{m,x}$, $S_{m,y}$, and $S_{m,z}$ are the source terms for *x, y* and *z* component.

3 Results and Discussion

3.1 Grid Independence Analysis

A grid independence analysis is an important part of this research in order to find an optimum number of mesh elements. This is required to ensure that the computational time taken are minimized while getting accurate results.

These analyses followed the grid independence analysis used by Halder et al. [14] to study flow over a few topographies. In Halder's study, the number of mesh elements was increased in successive models and simulation was carried out for each successive models at inlet velocities of 0.1 ms^{-1}. Wall shear stress was taken as the key parameter to determine the optimum number of mesh elements. The percentage difference the key parameter for each mesh refinement is then calculated to get the relative error. Relative error of less than 5% is acceptable for each successive models used in mesh refinements. Table 1 shows the grid independence analysis done in this research.

Table 1. Grid independence analysis of the models

3D model				Optimum number of mesh elements
Non-hierarchical	Mesh refinements	522171 → 2233727	2233727 → 6481004	2233727
	Relative error (%)	45.83	3.33	
Hierarchical	Mesh refinements	817734 → 1941795	1941795 → 2169321	1941795
	Relative error (%)	13.04	4.17	

3.2 CFD Results

3.2.1 Hagen-Poiseuille's Theory

The development of the flow follows the Hagen-Poiseuille's Theory. Figure 6 shows the development of the flow from the inlet to become a parabolic flow before it reaches the topography at YZ plane (z = 0). The velocity contour plot in Figure 6 shows that the flow has developed a fully parabolic flow before it reaching the topography array.

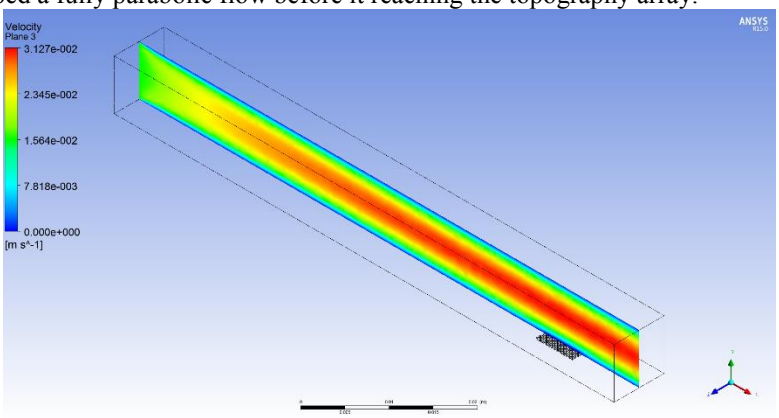

Fig. 6. The velocity contour plot at XY plane ($z = 0$)

This is further confirmed by the measured velocity profile of the fluid domain shown in Figure 7. A fully developed parabolic flow is proven where the maximum fluid velocity is located at the central height of the fluid domain and zero velocity at the walls of the domain. Both topography models in this research exhibits similar results.

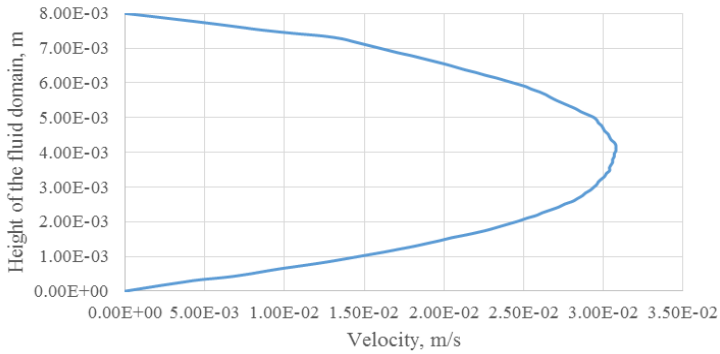

Fig. 7. Velocity profile before it reaches the topography

3.2.2 Velocity Streamlines and Vector Plot

Figures 8 shows streamlines for fluid flow over the non-hierarchical topography. The streamlines show that fluid flowing above the surface of the cube is moving at a faster speed. Fluid then flows into the gaps in between the cubes and exits the topography at a lower velocity. The average velocity above the gap is 4.41×10^{-4} ms^{-1}.

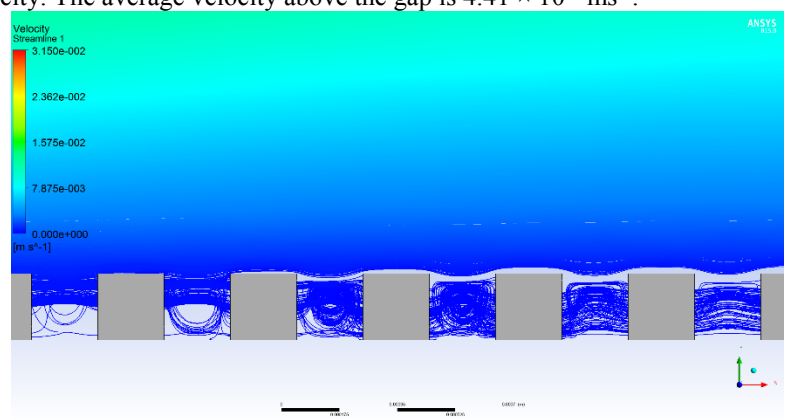

Fig. 8. Streamlines over non-hierarchical topographies

The vector plot profile shown in Figure 9 the fluid flow into the gaps at its lowest velocity and there is formation of vortices and slips. These vortices were rotating in clockwise direction in the gaps.

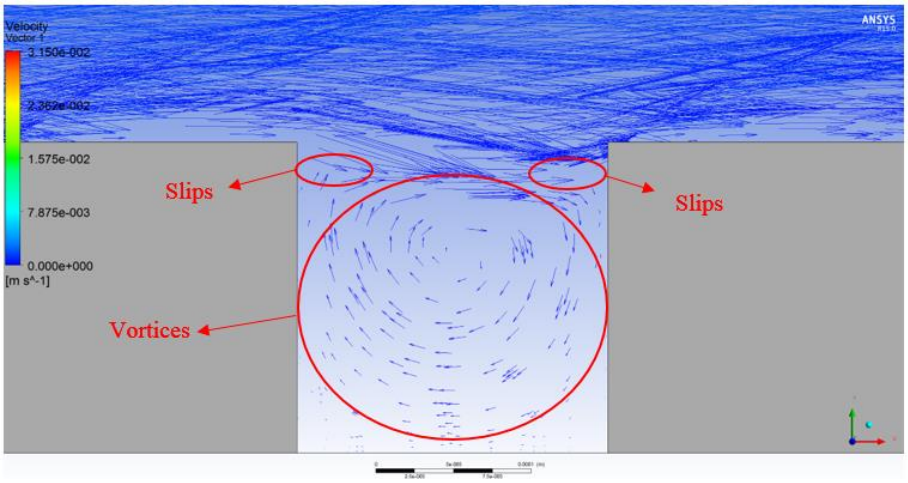

Fig. 9. Vector plot for non-hierarchical showing formation of vortices and slips

Figure 10 shows a streamlines plot for fluid flow through the hierarchical topography. The streamlines show that fluid flowing above the surface of the cube has higher speed and exits the topography array at a lower velocity. The characteristics of the flow is similar to non-hierarchical topography. However, the average velocity above the gap is 8.474×10^{-4} ms^{-1} which is higher than the average velocity of flow above the gaps of the non-hierarchical topography. This indicates the possibility of the hierarchical topography exhibiting better antifouling potential because flows at higher velocity would reduce the chances for prolonged exploration by biofouling organisms[18].

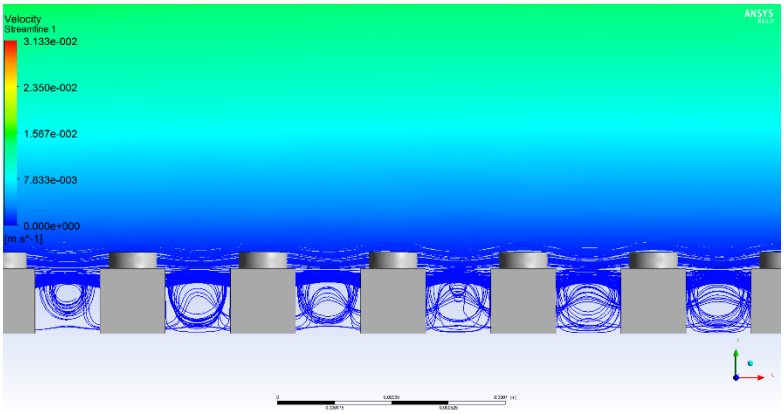

Fig. 10. Streamlines over hierarchical topographies

The vector profile in Figure 11 shows that fluid flow in gaps between topographical features is at the lowest velocity. There is also formations of vortices and slips. The vortices were rotating in clockwise direction in the gaps.

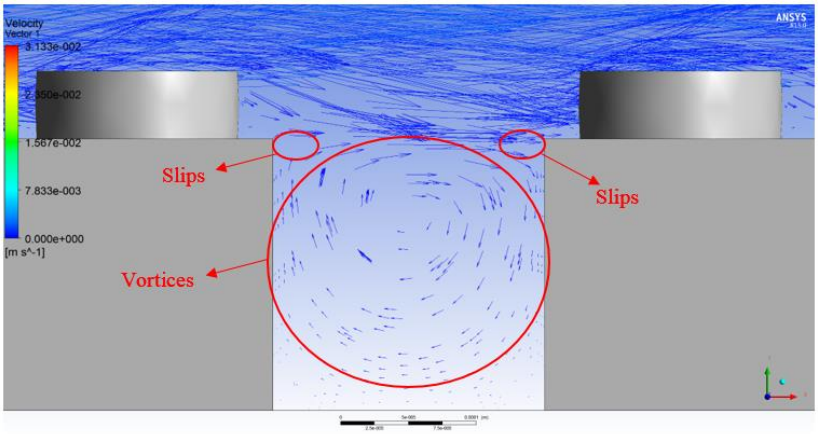

Fig. 11. Vector plot for non-hierarchical showing formation of vortices and slips

In a study conducted by Friedmann et. al [19], similar findings were found where there is formation of vortices in between the riblets. The redirection of the flow of the fluid into and out of the gaps between riblets had significantly decreased fluid velocity. The author also explained that the velocity of the fluid at the peaks of the riblets is high and causes it to slip over the fluid in between the riblets.

In this study, the findings are slightly similar to Friedmann's study. When the fluid flows through the topography, the fluid is redirected into the gaps in between these topographies. As a result, it causes interruption of the flow direction and there will be significant reduction of velocity in this area. Hence, there will be slip in between different layer of fluid flow with different velocities. Then, the vortices were formed as the slips force the fluid in the gaps to rotate [19].

Slips and vortices could possibly help microorganisms to settle in the gaps. This is because at this region, the velocity of the fluid is low which makes it favorable for the microorganisms or other biofouling material to settle and accumulate in this region. Since these gaps are not enclosed and there is fluid flowing around these spaces, there is a possibility for the biofouling materials to be brought out along with the flow that exists in the area.

3.2.3 Wall Shear Stress

Studies have shown substrates that are favorable for settlement and attachment tend to be explored at length by microorganisms. For instance, in a study conducted by Rosenhahn et al. [6], spinning action by algae spores at a place determines the strength of adhesion for permanent attachment. Therefore, biofouling can be prevented by reducing the contact between the microorganisms with the surface.

The possibility of the microorganisms to be detached from the surface can be measure by the wall shear stress. This is one of the crucial parameters in determining the antifouling potential of a surface [14], [20]. The shear stress of the adjacent fluid layer to the wall can be calculated by wall shear stress and it is induced by the velocity of the fluid flow over the topographies.

Figure 12 shows the wall shear stress distribution on the non-hierarchical topography. The highest wall shear stress can only be seen slightly at the edges on the first column from the right which is the first column of the topography being hit by the flow of fluid. There is less or minimal wall shear stress at the spaces in between the topographies. The middle and left most region shows similar wall shear stress which is low.

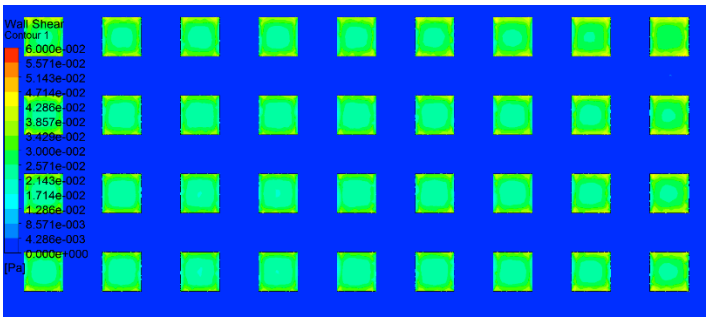

Fig. 32. Wall shear contour plot for non-hierarchical topography

Figure 13 shows the wall shear stress distribution on the hierarchical topography. The pattern of wall shear distribution is different from the non-hierarchical topography. It is observed that almost all edges of the circular pillars are experiencing higher degrees of shear stresses. There is also less or minimal wall shear stress at the spaces in between the topographies. It is important to notice that only the first column from the right shows the most edges with high wall shear stress as it is the first column to be hit by the flow of the fluid. Nevertheless, the wall shear stress distribution in Figures 12 and 13 shows that hierarchical topography has higher wall shear stress distribution compared to the non-hierarchical topography.

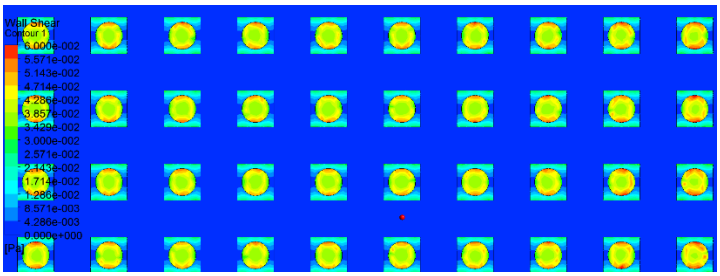

Fig. 43. Wall shear contour for hierarchical topography

Since hierarchical topography induce higher flow stresses, it is likely that this topography would exhibit better antifouling performance as compared to the non-hierarchical topography. High shear stresses is an important parameter in shearing off any microorganisms that is trying to attach to the substrates. Similar results were obtained in a study conducted by Lee et al. [21] where the antifouling performance of micro-sized prisms was investigated. In this study, the peaks of the prisms were less fouled in lab experiments as it exerts higher shear stress in CFD simulations [21].

Figure 14 shows a comparison of wall shear at the top of both hierarchical and non-hierarchical topographies. The graph shows that fluctuations of wall shear stress for the hierarchical surface is higher as compared to the non-hierarchical topography. This fluctuation of wall shear will help in preventing the settlement of biofouling material. The range for wall shear of hierarchical topography is between 0.00281 Pa and 0.00452 Pa while non-hierarchical topography is between 0.00165 Pa and 0.00301 Pa. The data clearly shows that the hierarchical topography has higher potential for antifouling applications.

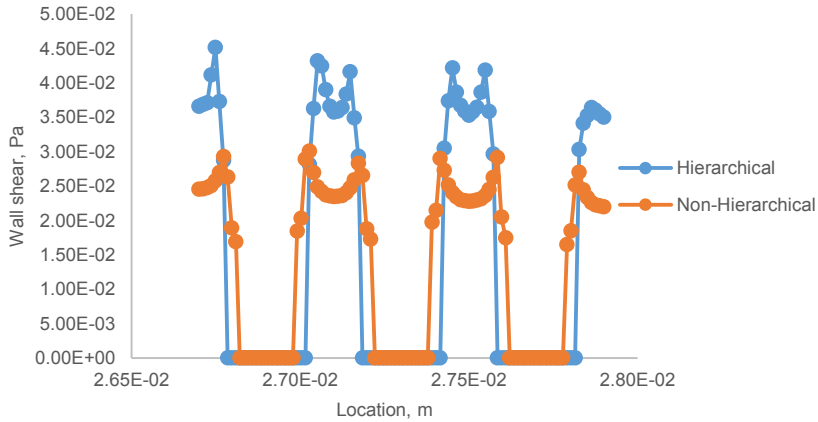

Fig. 14. Graph of wall shear for both topographies

4 Conclusion

The methodology of analysing the effect of hierarchical and non-hierarchical topography in controlling biofouling using CFD (ANSYS-CFX version 15, Solidworks 2013) has been demonstrated. The numerical method and boundary settings used in this study is sufficient to analyse the flow characteristics. This proved that numerical analysis is one of the best methods in studying the flow patterns over these topographies. It is shown that hierarchical topography has higher antifouling performance compared to non-hierarchical topography. This is because hierarchical topography has higher wall shear stress distribution compared to non-hierarchical topography. In addition, the flow characteristics of hierarchical topography indicates that it is superior in controlling biofouling compared to non-hierarchical topography.

References

1. H.-C. Flemming, "Biofouling in water systems--cases, causes and countermeasures." Appl. Microbiol. Biotechnol., **9**, no. 6, 629–40, (2002).
2. T. Vladkova, "Surface modification approach to control biofouling," in Marine and Industrial Biofouling, **7,** 135–163, (2009).
3. M. P. Schultz, J. a. Bendick, E. R. Holm, and W. M. Hertel, "Economic impact of biofouling on a naval surface ship," Biofouling, 27, **1**, 87–98, (2011).
4. R. Steinhagen, H. Müller-Steinhagen, and K. Maani, "Problems and Costs due to Heat Exchanger Fouling in New Zealand Industries," Heat Transf. Eng., **14**, (1993).
5. T. Vladkova, "Surface Engineering for non-toxic Biofouling Control," J. Univ. Chem. Technol. Metall., **42**, 239–256, (2007).
6. A. Rosenhahn and G. H. Sendra, "Surface sensing and settlement strategies of marine biofouling organisms," Biointerphases, **7**, 1–13, (2012).
7. K. A. Dafforn, J. A. Lewis, and E. L. Johnston, "Antifouling strategies: History and regulation, ecological impacts and mitigation," Mar. Pollut. Bull., **62**, 453–465, (2011).
8. Imo, "International Convention on the Control of Harmful Anti-Fouling Systems on Ships," Afs/Conf/26, **1,** 1–28, (2001).

9. P. E. Gibbs and G. W. Bryan, "Reproductive Failure in Populations of the Dog-Whelk, Nucella Lapillus, Caused by Imposex Induced by Tributyltin from Antifouling Paints," J. Mar. Biol. Assoc. United Kingdom, **66**, 767–777, (1986).
10. C. Alzieu, J. Sanjuan, P. Michel, M. Borel, and J. P. Dreno, "Monitoring and assessment of Butyltins in Atlantic coastal waters," *Mar. Pollut. Bull.*, **20**, 22–26, (1989).
11. J. A. Nichols, "Antifouling paints: Use on boats in San Diego Bay and a way to minimize adverse impacts," *Environ. Manage.*, **12**, 243–247, (1988).
12. Z. C. Xie, C. W. Nga, P. Y. Qian, and J. W. Qiu, "Responses of polychaete Hydroides elegans life stages to copper stress," Mar. Ecol. Prog. Ser., **285**, 89–96, (2005).
13. K. Schiff, D. Diehl, and A. Valkirs, "Copper emissions from antifouling paint on recreational vessels," Mar. Pollut. Bull., **48**, 371–377, (2004).
14. P. Halder *et al.*, "A novel approach to determine the efficacy of patterned surfaces for biofouling control in relation to its microfluidic environment," Biofouling, **29**, 697–713, (2013).
15. N. A. Mortensen, F. Okkels, and H. Bruus, "Reexamination of Hagen-Poiseuille flow: Shape dependence of the hydraulic resistance in microchannels," Phys. Rev. E - Stat. Nonlinear, Soft Matter Phys., **71**, (2005).
16. N. Aldred, A. Scardino, A. Cavaco, R. de Nys, and A. S. Clare, "Attachment strength is a key factor in the selection of surfaces by barnacle cyprids (Balanus amphitrite) during settlement.," Biofouling, **26**, 287–299, (2010).
17. P. M. Palaskar, "Effect of Side Taper on Aerodynamics Drag of a Simple Body Shape with Diffuser and without Diffuser MIRA Reference Car and Geometry," SAE Tech. Pap., **15**, 786-795, **(**2016).
18. J. F. Schumacher *et al.*, "Engineered antifouling microtopographies - effect of feature size, geometry, and roughness on settlement of zoospores of the green alga Ulva.," Biofouling, **23**, 55–62, (2007).
19. E. Friedmann, J. Portl, and T. Richter, "A study of shark skin and its drag reducing mechanism," in Advances in Mathematical Fluid Mechanics - Dedicated to Giovanni Paolo Galdi on the Occasion of His 60th Birthday, **50**, 271–285, (2010).
20. P. Halder *et al.*, "An assessment of the dynamic stability of microorganisms on patterned surfaces in relation to biofouling control.," Biofouling, **30**, 695–707, (2014).
21. Y. K. Lee, Y. J. Won, J. H. Yoo, K. H. Ahn, and C. H. Lee, "Flow analysis and fouling on the patterned membrane surface," J. Memb. Sci., **427**, 320–325, (2013).